Profile-Free Launch Point Estimation for Ballistic Targets using Passive Sensors

RATNASINGHAM THARMARASA
THIAGALINGAM KIRUBARAJAN
NANDAKUMARAN NADARAJAH
YAAKOV BAR-SHALOM
THAYANANTHAN THAYAPARAN

This paper considers the estimation of the Launch Points (LP) of ballistic targets from two or more passive satellite-borne sensors by fusing their angle-only measurements. The targets are assumed to have a two-stage boost phase with a free-flight phase between the two stages. Due to the passive nature of the sensors, there is no measurement during the free-flight motion. It is also assumed that measurements are available only after a few seconds from the launch time due to cloud cover. In the literature, profile-based methods have been proposed to estimate the target's launch point and trajectory. Profile-based methods normally result in large errors when there is a mismatch between actual and assumed profiles, which is the case in most scenarios. In this paper, a profile-free method is proposed to estimate the target states at the End-of-Burnout (EOB) and LP. Estimates at the EOB are obtained by using forward-filtering with adaptive model selection based on boost phase changes. The LP estimates are obtained using smoothing followed by backward prediction. Uncertainties in the motion model and the launch time must be incorporated in the backward prediction. The LP estimate and the corresponding error covariance are obtained by incorporating the above uncertainties. Simulation results illustrating the performance of the proposed approach are presented.

Manuscript received July 11, 2011; revised October 14, 2011; released for publication October 17, 2011.

Refereeing of this contribution was handled by Peter Willett.

Authors' addresses: R. Tharmarasa and T. Kirubarajan, McMaster University, Hamilton, ON, Canada, E-mail: (tharman@mail.ece.mcmaster.ca, kiruba@mcmaster.ca); N. Nandakumaran, Curtin University of Technology, Perth WA, Australia, E-mail: (n.nadarajah@curtin.edu.au); Y. Bar-Shalom, University of Connecticut, Storrs, CT, E-mail: (ybs@ee.uconn.edu); T. Thayaparan, Defence Research & Development Canada, Ottawa, ON, Canada, E-mail: (Thayananthan.Thayaparan@drdc-rddc.gc.ca).

1557-6418/12/$17.00

1. INTRODUCTION

Estimating the Launch Points (LP) of ballistic targets is an important problem in missile defence in order to take action against them. In the literature, profile-based and profile-free methods have been proposed to estimate the states of a target at end-of-burnout (EOB) and/or LP using active or passive sensors [6, 7, 12, 13, 22]. In profile-based methods, most model parameters are assumed to be known [12, 16]. In [12], a profile-based maximum likelihood estimation method was proposed to find the launch point estimate. In [21], estimating the launch parameters using an analytic approximation of the trajectory and an Unscented Kalman Filter (UKF) was analyzed. The profile-based methods will give good results when the model assumptions are accurate. However, when the model is poor, estimates of the profile-based methods will have large errors.

The influence of a priori uncertainties in launch time and trajectory profile on estimation of launch point using spaced-based infrared sensors was analyzed in [5]. In [22], the advantages of profile-free methods for EOB state estimation were explained with examples. The launch and impact point estimation of a ballistic target using radar measurements under different hypotheses on the available prior knowledge was studied in [3]. In that paper, nonlinear batch estimator combined with a recursive multiple model particle filter was proposed. In [10], the advantages of the Particle Filter (PF) over the Kalman Filter (KF) based Interacting Multiple Model (IMM) trackers for the launch point estimation of ballistic targets with single stage boost phase was analyzed. A launch point estimation algorithm using U-D factorization-based Kalman filter and Rauch-Tung-Striebel (RTS) smoother was proposed in [14].

In this paper, a profile-free method is proposed to estimate the LP of a ballistic target that has a two stage boost phase with a free-flight phase between the two phases. Two or more satellite-borne passive sensors, which measure the azimuth and elevation, are available to provide measurements. In most cases, an IMM filter will be a better choice to track a target with maneuvers. However, if the maneuver models and the times at which maneuvers occur are known, then a single model filter with time-varying model can be used instead of IMM. If there is no free-flight phase between two stages, it would be challenging to know the stage changes of the boost phase. Due to the passive nature of the sensors, no measurements will be obtained during the free-flight phase. Hence, the times at which boost phase's stage changes occur are known accurately. In this paper, a profile-free single time-varying model filter is proposed to estimate the states at EOB and LP.

The estimate of the target state at the first measurement time can be improved by performing smoothing with all available measurements. The first measurement will be typically received only after a few seconds from the launch time due to cloud cover. A backward predic-

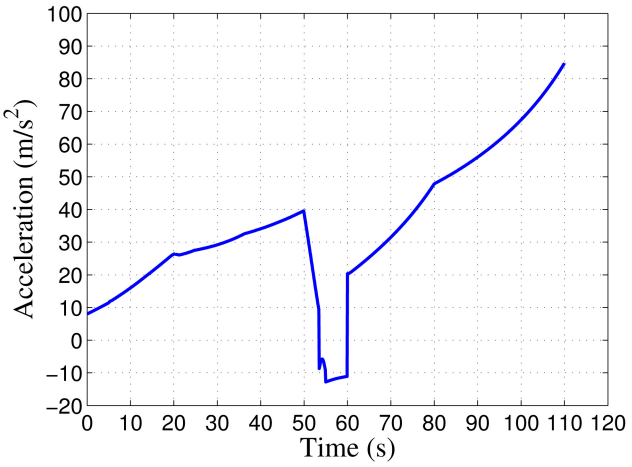

Fig. 1. Acceleration for a sample boost phase.

tion from first measurement time is needed to find the LP estimate. Uncertainties in the launch time and in the dynamic model must be considered while performing backward prediction. A least squares estimation method is proposed for the above backward prediction.

It is always beneficial to estimate the LP as soon as possible. However, the use of measurements over multiple time steps will improve the accuracy of the LP estimate. Due to motion model uncertainties and target maneuvers, measurements beyond a certain time might not add much information to the LP estimate. The Posterior Cramer-Rao Lower Bound (PCRLB) is a useful bound to predict the performance of an estimator [19, 20]. The contribution of the measurements over time to the EOB and LP state estimates can be evaluated using the PCRLB. Based on these PCRLBs, one can decide whether to use all available measurements over time or a subset of them in estimating the LP and EOB states. The PCRLB equations and values for simulations for forward filtering and smoothing are given in this paper.

The remainder of the paper is structured as follows. Section 2 describes the problem considered in this paper. The dynamic models used in the approach are given in Section 3. The profile-free estimation algorithm is explained in Section 4. Section 5 presents simulation results that demonstrate the effectiveness of the approach. Conclusions are presented in Section 6.

2. PROBLEM STATEMENT

The following assumptions are made:

- The target has a two-stage boost phase.
- There is a free-flight phase between the two stages of the boost phase.
- No measurements are available during the free-flight phase.
- No measurements are available for a few seconds from the launch time.

The acceleration magnitudes of a sample boost phase [4] are shown in Fig. 1. In this sample boost phase, the first boost stage is from $t_1 = 0$ to $t_2 = 55$ s and the second boost phase is from $t_3 = 60$ to $t_4 = 110$ s with a free-flight phase from $t_2 = 55$ to $t_3 = 60$ s. There is a continuous reduction in the acceleration from $t_2 - t_d = 50$ to $t_2 = 55$ s, where t_d is the first stage boost decay time.

Measurements are azimuth θ and elevation γ (in radians). The measurement equation for sensor j is given by

$$\mathbf{z}^j(k) = \begin{bmatrix} \theta^j(k) \\ \gamma^j(k) \end{bmatrix} = \underbrace{\begin{bmatrix} \text{atan}\left(\dfrac{y(k) - y_s^j(k)}{x(k) - x_s^j(k)}\right) \\ \text{atan}\left(\dfrac{z(k) - z_s^j(k)}{\sqrt{(x(k) - x_s^j(k))^2 + (y(k) - y_s^j(k))^2}}\right) \end{bmatrix}}_{h(\mathbf{x}_p(k), \mathbf{x}_s^j(k))} + w^j(k) \tag{1}$$

where (x, y, z) and (x_s^j, y_s^j, z_s^j) are the locations of the target and sensor j, respectively, $\mathbf{x}_p = [x \; y \; z]'$ is the target position vector, atan$(\cdot)$ is the four-quadrant arctangent, and $w^j(k)$ is a zero-mean Gaussian random variable with covariance $R^j(k)$.

3. DYNAMIC MODELS

The dynamic equation is given by

$$\mathbf{x}(k+1) = F(k)\mathbf{x}(k) + v(k) \tag{2}$$

where $\mathbf{x}(k)$ is the state vector, $F(k)$ is the state transition matrix, and $v(k)$ is zero-mean white noise with covariance $Q(k)$. The dynamic models used in this paper are given below.

3.1. White Noise Jerk model

This is also called Wiener Process Acceleration (WPA) model. In this model, the state vector comprises position, velocity, and acceleration. The state transition matrix $F(k)$ and process noise covariance $Q(k)$ (in one generic coordinate) are given by (this is the discretized continuous time model, CWPA) [2]

$$F(k) = \begin{bmatrix} 1 & T & T^2/2 \\ 0 & 1 & T \\ 0 & 0 & 1 \end{bmatrix} \tag{3}$$

and

$$Q(k) = q_m \begin{bmatrix} T^5/20 & T^4/8 & T^3/6 \\ T^4/8 & T^3/3 & T^2/2 \\ T^3/6 & T^2/2 & T \end{bmatrix} \tag{4}$$

where T is the sampling interval[1] at k, i.e., $T = t_{k+1} - t_k$, and q_m is the power spectral density (PSD) of the continuous time process noise (with dimension [length]^2/[time]^5).

[1]The sampling interval is assumed constant, but it can be variable, in which case T_k should be used in (3)–(8).

3.2 Wiener Process Jerk Model

In this model (WPJ), the state vector comprises position, velocity, acceleration, and jerk. The state transition matrix $F(k)$ and process noise covariance $Q(k)$ (in one generic coordinate) are given by (this is the discretized continuous time model, CWPJ)

$$F(k) = \begin{bmatrix} 1 & T & T^2/2 & T^3/6 \\ 0 & 1 & T & T^2/2 \\ 0 & 0 & 1 & T \\ 0 & 0 & 0 & 1 \end{bmatrix} \tag{5}$$

and

$$Q(k) = q_m \begin{bmatrix} T^7/252 & T^6/72 & T^5/30 & T^4/24 \\ T^6/72 & T^5/20 & T^4/8 & T^3/6 \\ T^5/30 & T^4/8 & T^3/3 & T^2/2 \\ T^4/24 & T^3/6 & T^2/2 & T \end{bmatrix} \tag{6}$$

where q_m is the PSD of the continuous time process noise (with dimension [length]^2/[time]^7).

3.3. Exponentially Autocorrelated Acceleration Model

This model is also called the Singer model. In this model, the state vector comprises position, velocity, and acceleration. The state transition matrix $F(k)$ and process noise covariance $Q(k)$ (in one generic coordinate) are given by [2, 11]

$$F(k) = \begin{bmatrix} 1 & T & (\alpha T - 1 + e^{-\alpha T})/\alpha^2 \\ 0 & 1 & (1 - e^{-\alpha T})/\alpha \\ 0 & 0 & e^{-\alpha T} \end{bmatrix} \tag{7}$$

and

$$Q(k) = 2\alpha\sigma_m^2 \begin{bmatrix} T^5/20 & T^4/8 & T^3/6 \\ T^4/8 & T^3/3 & T^2/2 \\ T^3/6 & T^2/2 & T \end{bmatrix} \tag{8}$$

where the acceleration autocorrelation is $E\{a(t)a(t+\tau)\} = \sigma_m^2 e^{-\alpha|\tau|}$. In the above, σ_m^2 is the instantaneous variance of the acceleration and $1/\alpha$ is the time constant of the target acceleration autocorrelation.

4. PROFILE-FREE ESTIMATION ALGORITHM

4.1. Track Initialization for Asynchronous Sensors

One-point initialization with the first measurement is used to initialize the target. Additional information other than the bearing and elevation measurements is needed to initialize the position in 3-D coordinates with a single measurement. It is reasonable to assume that the target's altitude will only be a few kilometers at the first detection time. Hence, the target altitude, $\hat{z}(1)$, is assumed to be $\hat{z}(1) = h_{\max}/2$ with variance $\sigma_h^2 = h_{\max}^2/12$, where $h_{\max}$ is the possible maximum altitude at the first measurement time. If the first measurement is received from sensor i, then the target's position is initialized as

$$\begin{bmatrix} \hat{x}(1) \\ \hat{y}(1) \\ \hat{z}(1) \end{bmatrix} = \begin{bmatrix} x_s^i(1) + \dfrac{(\hat{z}(1) - z_s^i(1))}{\tan(\gamma^i(1))}\cos(\theta^i(1)) \\ y_s^i(1) + \dfrac{(\hat{z}(1) - z_s^i(1))}{\tan(\gamma^i(1))}\sin(\theta^i(1)) \\ \dfrac{h_{\max}}{2} \end{bmatrix} \tag{9}$$

with covariance

$$P(1) = (\bar{H}^i(1)'\bar{R}^i(1)^{-1}\bar{H}^i(1))^{-1} \tag{10}$$

where $\bar{R}^i(1) = \text{diag}(R^i(1), \sigma_h^2)$ and

$$\bar{H}^i(1) = \frac{\partial \bar{h}(\mathbf{x}_p(1), \mathbf{x}_s^i(1))}{\partial \mathbf{x}_p(1)} \tag{11}$$

is the Jacobian matrix with elements

$$\bar{H}^i(1)(1,1) = -\frac{(\hat{y}(1) - y_s^i(1))}{(d_h^i)^2} \tag{12}$$

$$\bar{H}^i(1)(1,2) = \frac{(\hat{x}(1) - x_s^i(1))}{(d_h^i)^2} \tag{13}$$

$$\bar{H}^i(1)(1,3) = 0 \tag{14}$$

$$\bar{H}^i(1)(2,1) = \frac{-(\hat{z}(1) - z_s^i(1))(\hat{x}(1) - x_s^i(1))}{d_h^i (d_v^i)^2} \tag{15}$$

$$\bar{H}^i(1)(2,2) = \frac{-(\hat{z}(1) - z_s^i(1))(\hat{y}(1) - y_s^i(1))}{d_h^i (d_v^i)^2} \tag{16}$$

$$\bar{H}^i(1)(2,3) = \frac{d_h^i}{(d_v^i)^2} \tag{17}$$

$$\bar{H}^i(1)(3,1) = 0 \tag{18}$$

$$\bar{H}^i(1)(3,2) = 0 \tag{19}$$

$$\bar{H}^i(1)(3,3) = 1 \tag{20}$$

with

$$d_h^i = \sqrt{(\hat{x}(1) - x_s^i(1))^2 + (\hat{y}(1) - y_s^i(1))^2} \tag{21}$$

$$d_v^i = \sqrt{(\hat{x}(1) - x_s^i(1))^2 + (\hat{y}(1) - y_s^i(1))^2 + (\hat{z}(1) - z_s^i(1))^2}. \tag{22}$$

In the above, $\bar{h}(\mathbf{x}_p(1), \mathbf{x}_s^i(1))$ is the nonlinear measurement function for the stacked measurement $[\theta^i(1)\ \gamma^i(1)\ \hat{z}(1)]$

$$\bar{h}(\mathbf{x}_p(1), \mathbf{x}_s^i(1)) = \begin{bmatrix} h(\mathbf{x}_p(1), \mathbf{x}_s^i(1)) \\ \hat{z}(1) \end{bmatrix} \tag{23}$$

where $\hat{z}(1)$ is the measurement (prior information) of target altitude.

The target velocity, acceleration, and jerk estimates are initialized with mean zero and variances $(2v_{\max})^2/12$, $(2a_{\max})^2/12$, and $(2j_{\max})^2/12$, respectively, for the X and Y coordinates, and mean $v_{\max}/2$, $a_{\max}/2$, and $j_{\max}/2$ and variances $v_{\max}^2/12$, $a_{\max}^2/12$, and $j_{\max}^2/12$, respec-

tively, for the Z coordinate, where $v_{\max}$, $a_{\max}$, and $j_{\max}$ are the maximum possible velocity, acceleration and jerk, respectively. In the above, uniform distributions in $[-v_{\max}, v_{\max}]$, $[-a_{\max}, a_{\max}]$, and $[-j_{\max}, j_{\max}]$ are used for the X and Y coordinates, since their initial values can be positive or negative, while $[0, v_{\max}]$, $[0, a_{\max}]$, and $[0, j_{\max}]$ are used for the Z coordinate, since its initial values are always positive.

4.2. Track Initialization for Synchronized Sensors

If the sensors are synchronized, the initial target position is found using the Iterated Least Squares (ILS) estimator by fusing the measurements from all the sensors (configuration III fusion [1]). The estimate at iteration $j+1$ is given by

$$\hat{\mathbf{x}}_p^{j+1}(1) = \hat{\mathbf{x}}_p^{j}(1) + (\bar{\bar{H}}^{j'}(1)\bar{\bar{R}}^{-1}(1)\bar{\bar{H}}^{j}(1))^{-1}\bar{\bar{H}}^{j'}(1)\bar{\bar{R}}(1)^{-1} \times [\mathbf{z}(1) - \mathbf{h}(\hat{\mathbf{x}}_p^{j}(1), \mathbf{x}_s(1))] \tag{24}$$

where $\mathbf{z}(1) = [\mathbf{z}^1(1)\ \mathbf{z}^2(1) \cdots \mathbf{z}^n(1)]'$, n is the number of sensors, $\bar{\bar{R}}(1) = \text{diag}(R^1(1), R^2(1), \ldots, R^n(1))$,

$$\mathbf{h}(\mathbf{x}_p(1), \mathbf{x}_s(1)) = \begin{bmatrix} h(\mathbf{x}_p, \mathbf{x}_s^1) \\ h(\mathbf{x}_p, \mathbf{x}_s^2) \\ \vdots \\ h(\mathbf{x}_p, \mathbf{x}_s^n) \end{bmatrix} \tag{25}$$

and

$$\bar{\bar{H}}^{j}(1) = \left.\frac{\partial \mathbf{h}(\mathbf{x}_p(1), \mathbf{x}_s(1))}{\partial \mathbf{x}_p(1)}\right|_{\mathbf{x}_p(1)=\hat{\mathbf{x}}_p^{j}(1)} \tag{26}$$

is the Jacobian matrix, which is the stacked matrix with elements of ith block given by (12), (13), (15), and (16).

An initial estimate $\hat{\mathbf{x}}_p^0(1)$ for the ILS estimator is obtained from the intersection of the measurement from any one sensor with the earth's surface, as explained in section *Track Initialization for Asynchronous Sensors*.

The covariance of this (nonlinear) estimator[2] is

$$P(1) = (\bar{\bar{H}}(1)'\bar{\bar{R}}(1)^{-1}\bar{\bar{H}}(1))^{-1} \tag{27}$$

where $\bar{\bar{H}}$ is the last $\bar{\bar{H}}^{j}$ from (26).

The initial target velocity, acceleration, and jerk can also be estimated using a polynomial fit with composite measurements from the first few scans. The recursive filter can be started from $k = 1$ with a larger covariance than the polynomial fit indicates to avoid "double counting" the measurement information.

4.3. Forward Filtering

Since there is no measurement between the two stages of the boost phase, the times at which the boost stages are changing are known. If measurements are obtained during t_1 to t_2 and t_3 to t_4, then it is known that the target is under free-flight phase during t_2 to t_3. Absence of measurements for certain time period helps to know the boost phase transition. Hence, there is no need to use an IMM here.

For asynchronous sensors, an Extended Kalman Filter (EKF) is used to handle the nonlinearity in the measurement equation using sequential updating (configuration IV fusion [1]). For synchronized sensors, the EKF can be replaced with a Kalman Filter by finding composite measurements (i.e., complete target positions) from the azimuth and elevation measurements of all the sensors [1]. Composite measurements can be obtained using the ILS estimator, as explained in section *Track Initialization for Synchronized Sensors*. The target's dynamic model is adaptively changed based on the boost phase changes, which are known from the absence of measurements during the free-flight motion. A Wiener process jerk model is used during $[t_1, t_2 - t_d]$, where t_d is the time the target takes to go to free-flight phase from full acceleration of the first stage of the boost phase (decay time). During $[t_2 - t_d, t_2]$, a white-noise jerk model is used with large process noise, whose variance is calculated based on the estimated acceleration at time $t_2 - t_d$ and the acceleration of free-flight phase ($\ddot{x} = 0$, $\ddot{y} = 0$ and $\ddot{z} = -g$, where g is the gravitational acceleration of the earth, assumed constant). In one generic coordinate, the standard deviation of the process noise is set as $(a_{t_2 - t_d} - a_{t_2})/t_d$, where a is the acceleration. A white-noise jerk model with zero (or very small) process noise is used during $[t_2, t_3]$. Again, during $[t_3, t_4]$, a Wiener process jerk model is used.

The exact value of t_d is not known to the tracker. A white noise acceleration model with large process noise will work in $[t_2 - t_d, t_2]$ even if the actual motion is Wiener process jerk model, but it is not true for the converse. Hence, a maximum possible duration is used for t_d.

The estimated target state and its covariance must be modified during the model transitions. For the model transition at $t_2 - t_d$, i.e., Wiener process jerk model to white-noise jerk model, the jerk estimates and the corresponding covariances are removed. For the model transition at t_2, i.e., white-noise jerk model with large process noise to white-noise jerk model with zero or very small process noise, the acceleration estimates are changed to $\ddot{x} = 0$, $\ddot{y} = 0$ and $\ddot{z} = -g$, and the variances of the acceleration estimates are set to zero (or very small). For the model transition at t_3, the acceleration estimates are set to zero and the variances of the acceleration estimates are set to $(a_{\max}/2)^2$. Similarly, the jerk estimates are set to zero with variance $(j_{\max}/2)^2$.

A constrained Kalman Filter can be used to impose a minimum acceleration, which will help improve the tracking accuracy [18]. A directional process noise can

[2]This covariance is based on the CRLB. However, as shown in [17], this estimator is statistically efficient, i.e., the CRLB yields the actual covariance.

also be used based on the estimated velocity to reduce the uncertainty in the target motion.

The Wiener process jerk model can be replaced with an exponentially autocorrelated acceleration model. However, an accurate value of α must be known to get better estimates. The comparison of Wiener process jerk model and autocorrelated acceleration model is given in the simulation section.

The sequential updating technique, i.e., update of the target state with the measurement of one sensor at a time, is used to handle measurements from multiple sensors [1].

4.4. LP Estimation using Smoothing

After getting the estimate at EOB using forward filtering, smoothing is applied to find the estimate of the launch point. The smoothing can be performed back to the first measurement time as follows [2]

$$\hat{\mathbf{x}}(k \mid N) = \hat{\mathbf{x}}(k \mid k) + C(k)[\hat{\mathbf{x}}(k+1 \mid N) - \hat{\mathbf{x}}(k+1 \mid k)] \quad (28)$$

$$P(k \mid N) = P(k \mid k) + C(k)[P(k+1 \mid N) - P(k+1 \mid k)]C(k)' \quad (29)$$

for $k = N-1, \ldots, 2, 1$. In the above equation,

$$C(k) = P(k \mid k)F(k)'P(k+1 \mid k)^{-1}. \quad (30)$$

Since only one model is used at a time during the forward filtering, there is no need for IMM smoothing here. However, if multiple models are used, then the algorithm proposed in [15] must be used for smoothing with IMM.

The covariance of the smoothed estimates minus the covariance of the unsmoothed estimates must be negative semidefinite. Otherwise, from (29), the smoothed covariances become larger and larger with the backward iteration. If backward transition modifications are performed as the forward transitions, the smoothed variances of the jerk and/or acceleration become larger than their unsmoothed variances. Hence, backward transitions are handled as follows:

1) Wiener process jerk model to free-flight model (white noise jerk model with very small noise and known accelerations) backward transition (at t_3):
   - the smoothed accelerations are set to $[0 \;\; 0 \;\; -g]$.
   - the covariance is modified using (29) with $F = 12 \times 9$ matrix of zeros except

$$F(1,1) = F(2,2) = F(3,3) = F(5,4) = F(6,5) = F(7,6) = F(9,7) = F(10,8) = F(11,9) = 1 \quad (31)$$

   and $Q = 12 \times 12$ matrix of zeros except

$$Q(3,3) = Q(7,7) = Q(11,11) = (a_{\max}/2)^2 \quad (32)$$

$$Q(4,4) = Q(8,8) = Q(12,12) = (j_{\max}/2)^2. \quad (33)$$

   In (29), $P(k+1 \mid k)$ is found using the above F and Q matrices as

$$P(k+1 \mid k) = FP(k)F' + Q \quad (34)$$

   where k and $k+1$ indicate before and after the transition, respectively.

2) Free-flight model to white noise jerk model backward transition (at t_2):
   - if it is assumed that there is no sudden jump in the acceleration during this transition, then no modification is needed.
   - if a possible jump is assumed in the acceleration, then
     — the smoothed acceleration estimates are set to the forward filter estimates at the transition time, and
     — the covariance is modified using (29) with $F = 9 \times 9$ identity matrix and $Q = 9 \times 9$ matrix of zeros except

$$Q(3,3) = Q(6,6) = Q(9,9) = (a_{\max}/2)^2. \quad (35)$$

3) White noise jerk model to Wiener process jerk model backward transition (at $t_2 - t_d$):
   - the smoothed jerk estimates are set to the forward filter estimates at the transition time, and
   - the covariance is modified using (29) with $F = 9 \times 12$ matrix of zeros except

$$F(1,1) = F(2,2) = F(3,3) = F(4,5) = F(5,6) = F(6,7) = F(7,9) = F(8,10) = (9,11) = 1 \quad (36)$$

   and $Q = 9 \times 9$ matrix of zeros.

Finding the LP estimate using backward prediction from the smoothed estimate at the first measurement time (t_1) is difficult for the following reasons:

- The exact target dynamics, which may have multiple legs with different motion models, are unknown.
- It is possible to have abrupt changes in the acceleration.
- Flying time before the first measurement is unknown.

Uncertainties in the LP estimation can be reduced by using the following additional information:

- The velocity of the target is zero at the launch time.
- The altitude is nearly zero (or a known value based on the local topography) at launch time.

For the LP estimation using the smoothed state $\hat{\mathbf{x}}(1 \mid K)$, the state to be estimated is the state at LP, $\mathbf{x}(0)$, and the "measurement" is $\hat{\mathbf{x}}(1 \mid K)$. Then, the measurement equation for the X coordinate is

$$\underbrace{\begin{bmatrix} \hat{x}(1 \mid K) \\ \hat{\dot{x}}(1 \mid K) \\ \hat{\ddot{x}}(1 \mid K) \\ \hat{\dddot{x}}(1 \mid K) \end{bmatrix}}_{b_x} = \begin{bmatrix} 1 & T & T^2/2 & T^3/6 \\ 0 & 1 & T & T^2/2 \\ 0 & 0 & 1 & T \\ 0 & 0 & 0 & 1 \end{bmatrix} \begin{bmatrix} x(0) \\ 0 \\ \ddot{x}(0) \\ \dddot{x}(0) \end{bmatrix} + v_x(0) + \omega_x(1) \tag{37}$$

$$= \underbrace{\begin{bmatrix} 1 & T^2/2 & T^3/6 \\ 0 & T & T^2/2 \\ 0 & 1 & T \\ 0 & 0 & 1 \end{bmatrix}}_{A_x} \underbrace{\begin{bmatrix} x(0) \\ \ddot{x}(0) \\ \dddot{x}(0) \end{bmatrix}}_{\mathbf{x}_{\mathrm{LP}_x}} + v_x(0) + \omega_x(1) \tag{38}$$

where $v_x(0)$ is the process noise from launch time to the first measurement time and $\omega_x(1)$ is the "measurement noise" (error in $\hat{\mathbf{x}}(1 \mid K)$), whose covariance is the smoothed estimate's covariance of the X coordinate state at the first measurement time.

A similar equation is used for the Y coordinate. For the Z coordinate,

$$\underbrace{\begin{bmatrix} \hat{z}(1 \mid K) \\ \hat{\dot{z}}(1 \mid K) \\ \hat{\ddot{z}}(1 \mid K) \\ \hat{\dddot{z}}(1 \mid K) \end{bmatrix}}_{b_z} = \begin{bmatrix} 1 & T & T^2/2 & T^3/6 \\ 0 & 1 & T & T^2/2 \\ 0 & 0 & 1 & T \\ 0 & 0 & 0 & 1 \end{bmatrix} \begin{bmatrix} 0 \\ 0 \\ \ddot{z}(0) \\ \dddot{z}(0) \end{bmatrix} + v_z(0) + \omega_z(1) \tag{39}$$

$$= \underbrace{\begin{bmatrix} T^2/2 & T^3/6 \\ T & T^2/2 \\ 1 & T \\ 0 & 1 \end{bmatrix}}_{A_z} \underbrace{\begin{bmatrix} \ddot{z}(0) \\ \dddot{z}(0) \end{bmatrix}}_{\mathbf{x}_{\mathrm{LP}_z}} + v_z(0) + \omega_z(1). \tag{40}$$

Since there is no measurement available from the launch time to the first measurement time, the target can be backward-predicted in the X, Y, and Z coordinates separately only if the measurement noises are uncorrelated among coordinates. However, the covariance of the smoothed estimate $\hat{\mathbf{x}}(1 \mid K)$ will have non-zero values for cross-covariance between coordinates. Hence, the above equations for the X, Y, and Z coordinates must be stacked to find the correct least squares estimate.

The least squares estimate of LP is then given by

$$\hat{\mathbf{x}}_{\mathrm{LP}} = (A'\Sigma^{-1}A)^{-1}A'\Sigma^{-1}b \tag{41}$$

where $\mathbf{x}_{\mathrm{LP}} = [\mathbf{x}'_{\mathrm{LP}_x}\ \mathbf{x}'_{\mathrm{LP}_y}\ \mathbf{x}'_{\mathrm{LP}_z}]'$, $A = \mathrm{diag}(A_x, A_y, A_z)$, $b = [b'_x\ b'_y\ b'_z]'$, and Σ is the sum of the covariance of the smoothed estimate at the first measurement time and the covariance Q_0 of the process noise $v(0)$.

The covariance of the least squares estimate is given by

$$\mathrm{cov}(\hat{\mathbf{x}}_{\mathrm{LP}}) = (A'\Sigma^{-1}A)^{-1}. \tag{42}$$

In the above covariance calculation, launch time is assumed to be known. However, there is uncertainty in T, hence in A.

To include the uncertainty in T, T is stacked with the state vector to yield the augmented state $\mathbf{y}_{\mathrm{LP}} = [\mathbf{x}'_{\mathrm{LP}}\ T]'$. Since this is a nonlinear least squares problem, the ILS approach, as described in section 4.2, is used to estimate the launch point. The linearized measurement matrix becomes

$$\bar{A} = \begin{bmatrix} 1 & T^2/2 & T^3/6 & 0 & 0 & 0 & 0 & 0 & \ddot{x}(0)T + \dddot{x}(0)T^2/2 \\ 0 & T & T^2/2 & 0 & 0 & 0 & 0 & 0 & \ddot{x}(0) + \dddot{x}(0)T \\ 0 & 1 & T & 0 & 0 & 0 & 0 & 0 & \dddot{x}(0) \\ 0 & 0 & 1 & 0 & 0 & 0 & 0 & 0 & 0 \\ 0 & 0 & 0 & 1 & T^2/2 & T^3/6 & 0 & 0 & \ddot{y}(0)T + \dddot{y}(0)T^2/2 \\ 0 & 0 & 0 & 0 & T & T^2/2 & 0 & 0 & \ddot{y}(0) + \dddot{y}(0)T \\ 0 & 0 & 0 & 0 & 1 & T & 0 & 0 & \dddot{y}(0) \\ 0 & 0 & 0 & 0 & 0 & 1 & 0 & 0 & 0 \\ 0 & 0 & 0 & 0 & 0 & 0 & T^2/2 & T^3/6 & \ddot{z}(0)T + \dddot{z}(0)T^2/2 \\ 0 & 0 & 0 & 0 & 0 & 0 & T & T^2/2 & \ddot{z}(0) + \dddot{z}(0)T \\ 0 & 0 & 0 & 0 & 0 & 0 & 1 & T & \dddot{z}(0) \\ 0 & 0 & 0 & 0 & 0 & 0 & 0 & 1 & 0 \end{bmatrix}. \tag{43}$$

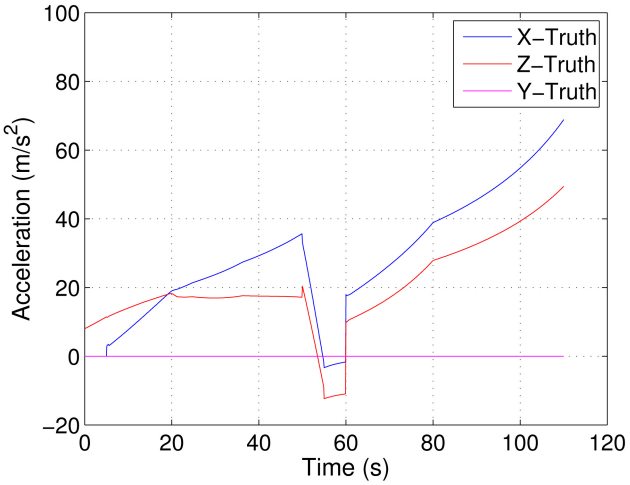

Fig. 2. Boost phase acceleration in each coordinate.

The estimate at iteration $j+1$ is given by

$$\hat{\mathbf{y}}_{\mathrm{LP}}^{j+1} = \hat{\mathbf{y}}_{\mathrm{LP}}^{j} + (\bar{A}'\Sigma^{-1}\bar{A})^{-1}\bar{A}'\Sigma^{-1}[b - \bar{A}\hat{\mathbf{y}}_{\mathrm{LP}}^{j}]. \quad (44)$$

An initial estimate $\hat{\mathbf{y}}_{\mathrm{LP}}^{0}$ for the ILS estimator is obtained using (41) with an assumed T.

The covariance of the iterative least squares estimate with uncertainty in the launch time is

$$\mathrm{cov}(\hat{\mathbf{y}}_{\mathrm{LP}}) = (\bar{A}'\Sigma^{-1}\bar{A})^{-1}. \quad (45)$$

Without any additional constraints, the solution of (44) might converge to a wrong estimate if the initial guess for the launch time is not close to the actual value. The solution can be improved by adding additional constraints for the accelerations

$$\mathrm{sign}(\hat{\ddot{x}}(1 \mid K)) = \mathrm{sign}(\ddot{x}(0)) \quad (46)$$

$$\mathrm{sign}(\hat{\ddot{y}}(1 \mid K)) = \mathrm{sign}(\ddot{y}(0)) \quad (47)$$

$$\mathrm{sign}(\hat{\ddot{z}}(1 \mid K)) = \mathrm{sign}(\ddot{z}(0)). \quad (48)$$

The above constraints say that the direction of the acceleration must be same as the direction of the velocity component of b. A constrained nonlinear least squares algorithm is required to solve the above problem [9]. MATLAB "fmincon" function can be used to solve the above problem.

4.5. Posterior Cramer-Rao Lower Bound

The PCRLB, which is defined as the inverse, $J(k)^{-1}$, of the Fisher Information Matrix (FIM), gives a lower bound on the error covariance [20]

$$E\{[\hat{\mathbf{x}}(k) - \mathbf{x}(k)][\hat{\mathbf{x}}(k) - \mathbf{x}(k)]'\} \geq J(k)^{-1} \quad (49)$$

where E denotes expectation over $(\mathbf{x}(k), Z(k) = [z(1), z(2), \ldots, z(k)])$.

For a system with a linear dynamic model and a nonlinear measurement model without measurement origin uncertainty, $J(k+1)$ can be written as [8]

$$J(k+1) = [Q(k) + F(k)J(k)^{-1}F(k)']^{-1} + \sum_{i=1}^{n} E(H^i(k)'R^i(k)^{-1}H^i(k)) \quad (50)$$

with the (m,n)th element of matrix $H_i(k)$ being given by

$$[H^i(k)](m,n) = \frac{\partial[h^i(k)](m)}{\partial \mathbf{x}(k)(n)}. \quad (51)$$

The PCRLB for smoothing without measurement origin uncertainty is the same as (29) [19].

During model transitions, the PCRLB can be modified in the same manner as the covariance modifications discussed in the forward filtering and smoothing sections.

5. SIMULATION RESULTS

The simulation settings are as follows:

- Target launch location at $T_0 = 0$ is 30°N latitude, 45°E longitude and 0 m altitude with heading east.
- First measurement is received 20 s after launch.
- The sampling interval is 0.2 s.
- The measurement error standard deviation (azimuth and elevation) is 10 μrad.
- Two IR sensors located on geostationary satellites.
  —Satellite 1 located at time T_0 is: 0° latitude, 5°W longitude and 37000 km altitude.
  —Satellite 2 located at time T_0 is: 0° latitude, 60°E longitude and 37000 km altitude.
- Measurements are synchronized between the two satellites.

The target trajectory is based on real data [4] and measurements are generated using simulation. The net acceleration magnitude of the target is shown in Fig. 1. Acceleration in each coordinate is shown in Fig. 2. During the free-flight motion, the acceleration is assumed to be $[0, 0, -10]$ m/s^2, however the actual values of the acceleration in the X-direction vary from -3.3 to -1.7 m/s^2 and in the Z-direction vary from -12.3 to -11 m/s^2. The atmospheric drag, which acts opposite to the target velocity vector, is the reason for the mismatch between the assumed and the actual accelerations. There is no mismatch in the acceleration in the Y-direction, since the velocity, hence drag, in that direction is zero. The first stage boost decay time t_d is assumed to be 5 s. A possible jump was assumed in the acceleration during the model transition at t_2. A constrained Kalman Filter is used to impose a minimum acceleration with $\ddot{x}_{\min} = -2$ m/s^2, $\ddot{y}_{\min} = -2$ m/s^2 and $\ddot{z}_{\min} = -12$ m/s^2.

5.1. EOB Estimate

The ground truth and estimates of the position of the targets from a sample run are shown in Fig. 3. Fig. 4 shows a magnified plot of Fig. 3 around the first measurement time. The velocity, acceleration, and

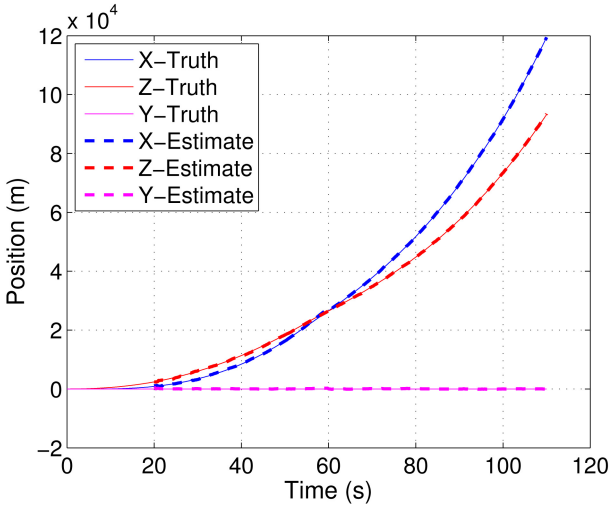

Fig. 3. Position estimates from a sample run.

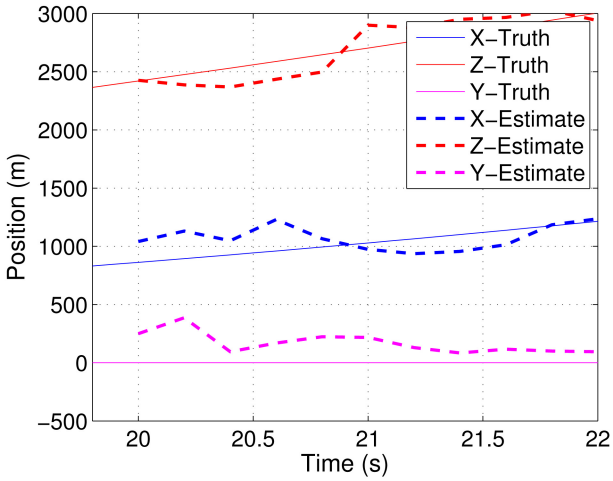

Fig. 4. Magnified plot of position estimates around the first measurement time.

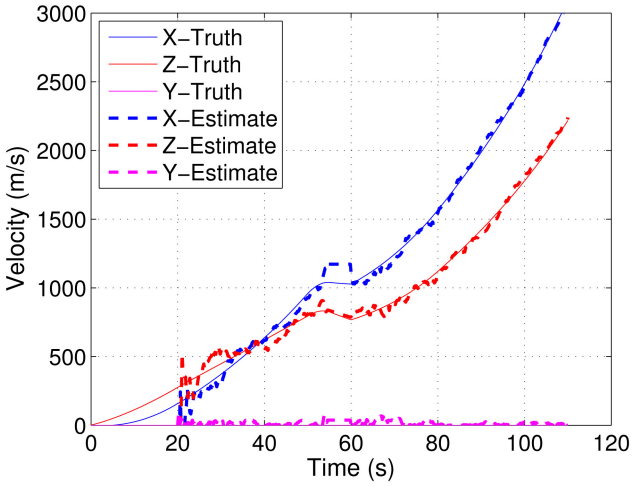

Fig. 5. Velocity estimates from a sample run.

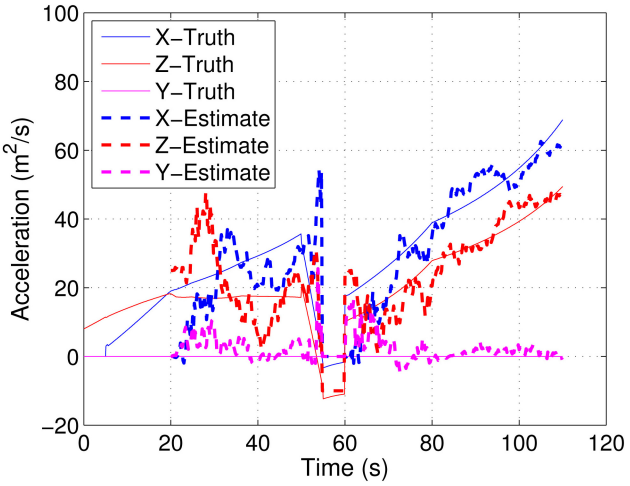

Fig. 6. Acceleration estimates from a sample run.

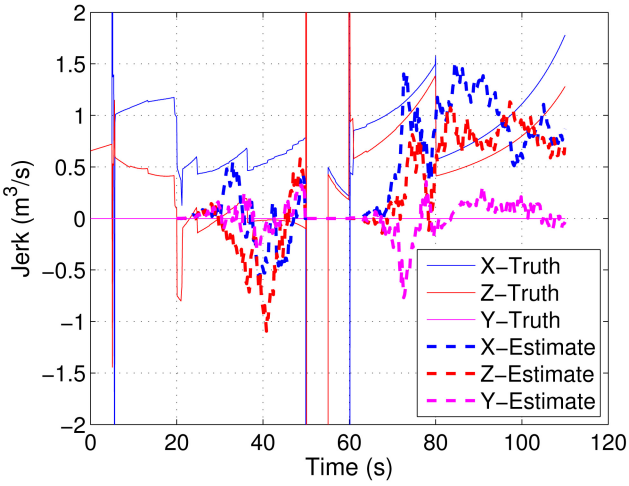

Fig. 7. Jerk estimates from a sample run.

jerk estimates from a sample run are shown in Figs. 5, 6, and 7, respectively. Due to insufficient measurement accuracy and short sampling duration, the acceleration reduction of the target during the time 50 s to 55 s is not estimated accurately. Jerk estimates are also not accurate. Even though jerk estimates are not accurate, the position, velocity and acceleration estimates are reasonably accurate.

The Root Mean Square Error (RMSE) values of position estimates calculated from 100 Monte-Carlo runs are shown in Fig. 8. When all the measurements are used, the RMSE at the EOB is around 125 m. Position RMSE is continuously increasing from time 55 s to 60 s because of absence of measurements and mismatch between assumed and actual acceleration. The position RMSE with the measurements of the second stage of the boost phase of the target is also shown in Fig. 8. The corresponding velocity RMSE is shown in Fig. 9. From these figures, it can be noticed that due to the high uncertainty in the acceleration and jerk at the start of second stage of the boost phase and high process noise, information from 20 s to 50 s did not give any improvement to the RMSE of the EOB state estimate. Position and velocity PCRLBs at EOB with measurements of different start times are shown in

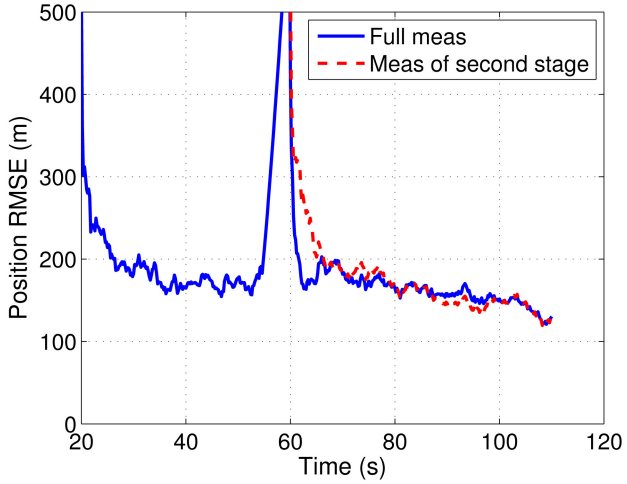

Fig. 8. EOB RMSE of position estimates with all measurements versus only measurements after 60 seconds.

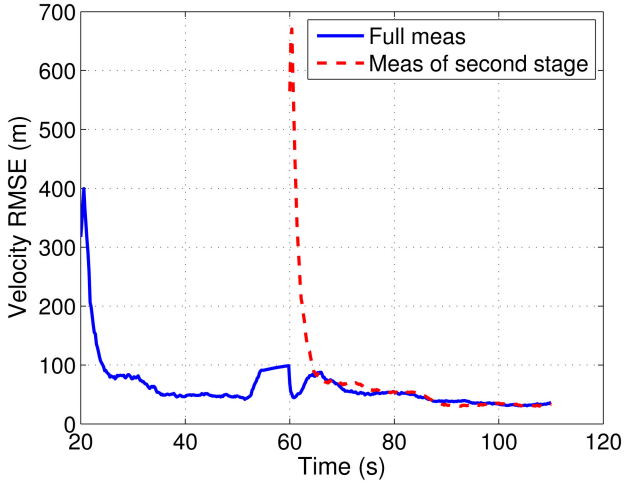

Fig. 9. EOB RMSE of velocity estimates with all measurements versus only measurements after 60 seconds.

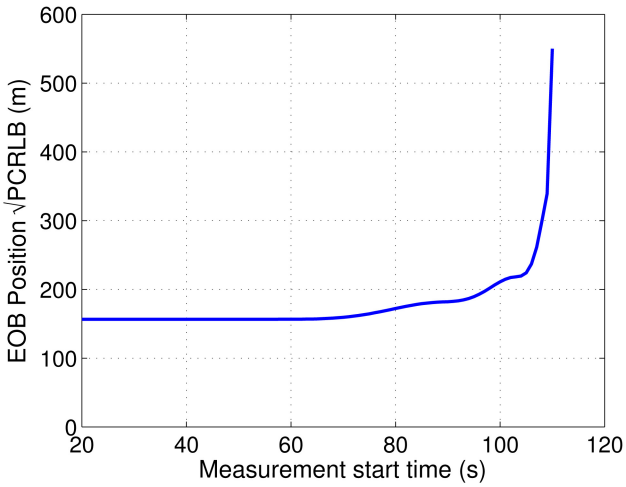

Fig. 10. Square root of position PCRLB of EOB state estimate with different measurement start time.

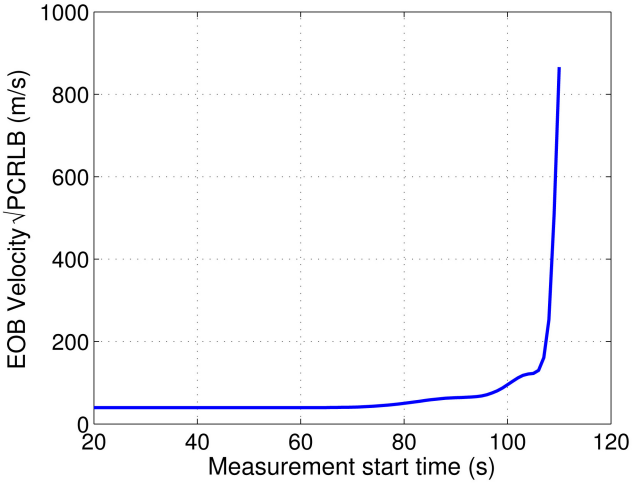

Fig. 11. Square root of velocity PCRLB of EOB state estimate with different measurement start time.

Figs. 10 and 11, respectively. From these two figures, it can be noticed that the measurements before 65 s do not add significant information to EOB state estimate.

5.2. LP Estimate

As expected, smoothed velocity, acceleration and jerk estimates are better than the filtered estimates without smoothing, as shown in Figs. 12, 13, and 14. Position and velocity RMSEs are also significantly improved by smoothing, as shown in Figs. 15 and 17. Since the velocity at the LP is assumed to be zero, there was no need to estimate it. As a result, the velocity RMSE is close to zero. The position RMSE at LP is around 500 m, which is a reasonable value for launch point estimation problem. The position RMSE of the launch point estimate is much higher than the estimate at the first measurement time (20 s), since no measurements were available from 0 s to 20 s. Figs. 16 and 18 show the PCRLB values corresponding to position and velocity RMSEs, respectively. The PCRLB and RMSE values are similar except at LP. The lower PCRLB compared to the RMSE at LP could be due to model mismatch.

The position and velocity RMSE of the smoothed estimates with measurements from first stage of boost phase of the target are shown in Figs. 19 and 20, respectively. From these figures it can be noticed that the measurements from the second stage of the boost phase do not contribute significantly to the LP estimation due to the sudden changes in acceleration and jerk during stage transition and the high process noises. Position PCRLBs of LP estimate using measurements with different end times are shown in Fig. 21. From this figure it can be noticed that the measurements after 50 s do not add significant information to LP estimate.

The comparison of the Wiener process jerk model with exponentially autocorrelated acceleration model is shown in Figs. 22 and 23. In this comparison, the following values are used for α: $\alpha_x = -0.02$, $\alpha_y = -0.02$, $\alpha_z = -0.01$. Except for the LP estimate, the RMSEs of both models are almost at the same level, since both

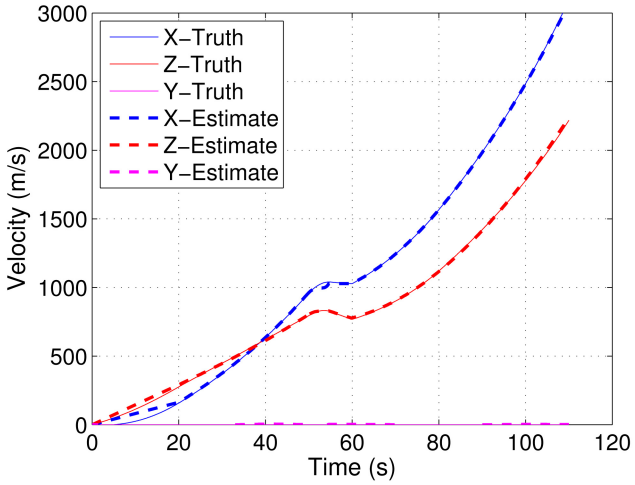

Fig. 12. Smoothed estimates of velocity from a sample run.

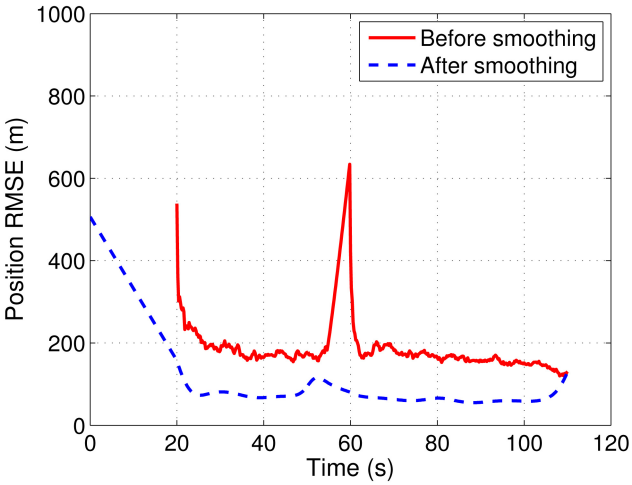

Fig. 15. Position RMSE.

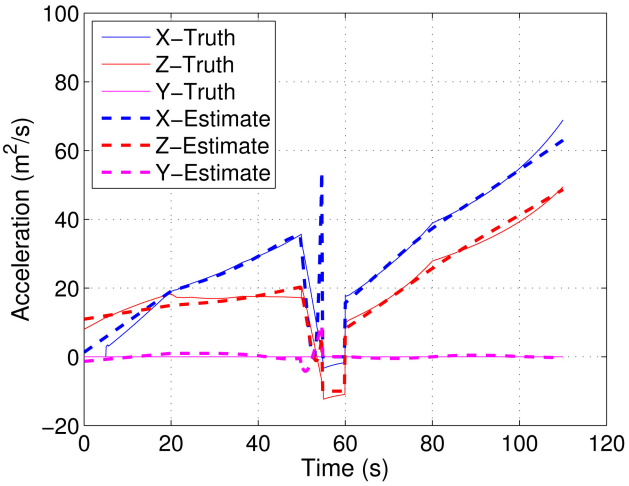

Fig. 13. Smoothed estimates of acceleration from a sample run.

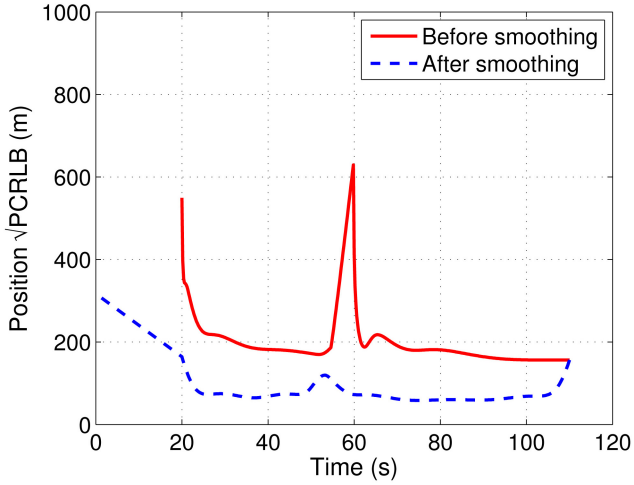

Fig. 16. Square root of position PCRLB.

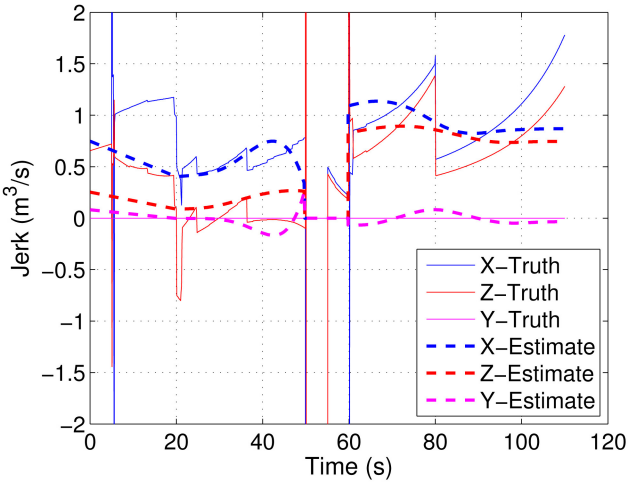

Fig. 14. Smoothed estimates of jerk from a sample run.

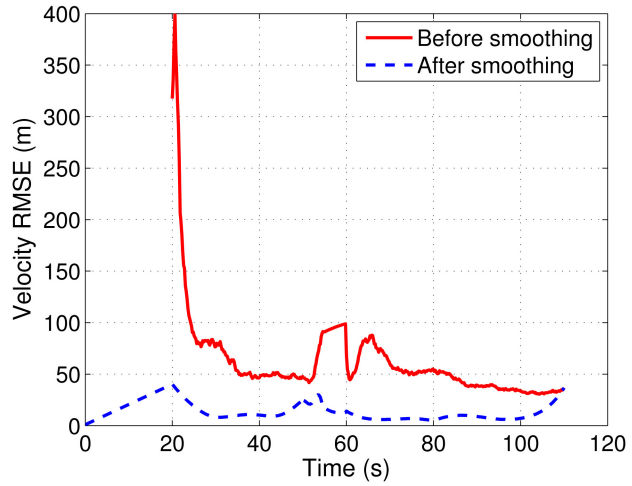

Fig. 17. Velocity RMSE.

models have almost the same error in approximating the actual model.

The RMSE, bias, and Standard Deviation (STD) of the LP estimate with the Wiener process jerk model and the exponentially autocorrelated acceleration model are shown in the columns two to five of Table I. The value of covariance Q_0 of the process noise $v(0)$ is set using (6) with PSD $q_m = 0.01$ m^{2}s^{-7}. For the Wiener process

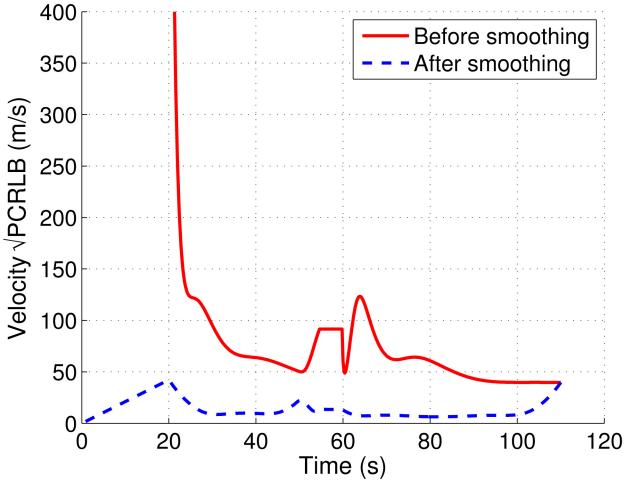

Fig. 18. Square root of velocity PCRLB.

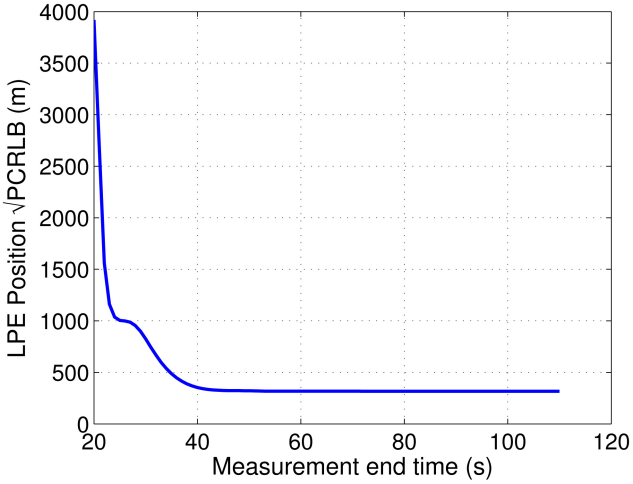

Fig. 21. Square root of position PCRLB of LP estimate with different measurement end time.

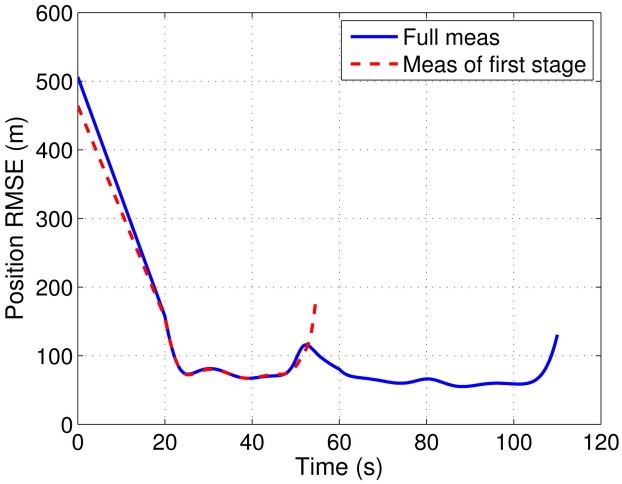

Fig. 19. RMSE of smoothed position estimates with all measurements versus only measurements of first stage of boost phase.

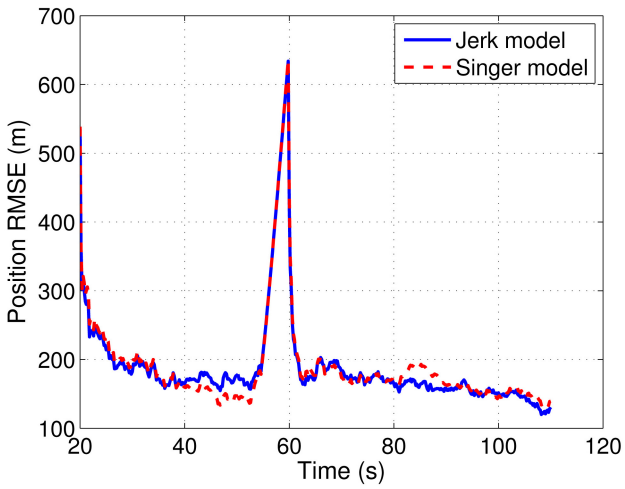

Fig. 22. RMSE of position estimates with Wiener process jerk model versus exponentially autocorrelated acceleration model.

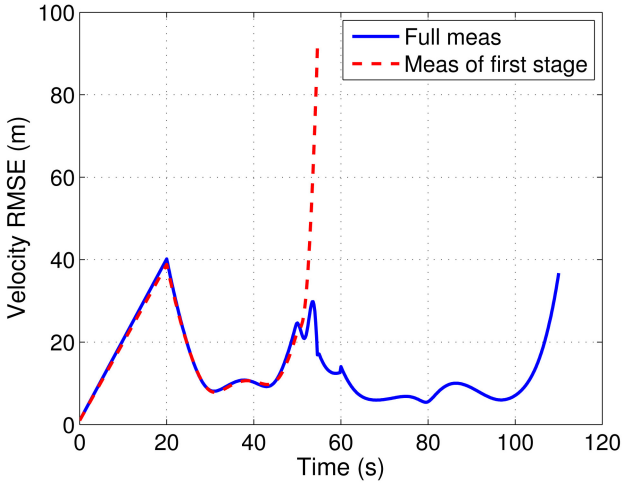

Fig. 20. RMSE of smoothed velocity estimates with all measurements versus only measurements of first stage of boost phase.

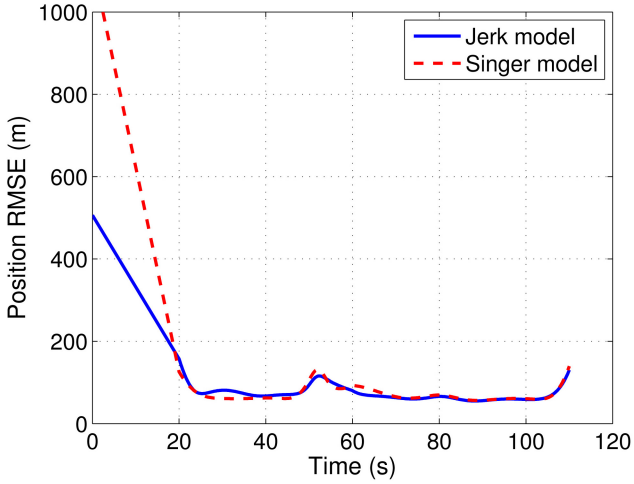

Fig. 23. RMSE of smoothed position estimates with Wiener process jerk model versus exponentially autocorrelated acceleration model.

TABLE I
Bias, RMSE and Standard Deviation of LP Estimate Calculated from 100 Monte-Carlo runs with 20 s Delay Before First Measurement

	CWPJ Model and Known Launch Time		Exponentially Autocorrelated Acceleration Model and Known Launch Time		CWPJ Model and Estimated Launch Time		CWPJ Model and Wrong Launch Time (assumed delay 25 s)	
	x (m)	y (m)	x (m)	y (m)	x (m)	y (m)	x (m)	y (m)
RMSE	376.97	185.50	855.98	112.53	368.72	130.71	381.53	273.07
Bias	−295.70	28.85	−846.41	6.10	−309.12	12.87	−170.46	52.49
STD	235.00	184.16	128.23	112.93	202.01	130.73	343.05	269.33

jerk model, the RMSE value in the X-direction is significantly larger than the STD due to the bias in the estimate. The bias in the estimate of the X coordinate is due to sudden change in the acceleration after 5 s from the launch (see Fig. 2), which introduces a model mismatch. For the exponentially autocorrelated acceleration model, the smoothed state's error standard deviation is reasonably small, however the RMSE values are large due to the large biases. These biases are due to the mismatch between the actual and used α values. It is very difficult to estimate a value for α in the time duration 0 to 20 seconds without any measurements.

So far, the launch time has been assumed known (i.e., the launch time is assumed first measurement time minus 20 s). When the launch time is unknown, the launch point estimation results obtained using MATLAB "fmincon" with constraints (46)–(46) are shown in the columns six and seven of Table I. The average of the launch time estimate $\hat{T}$ is 18.41 s. In order to analyze the effect of error in the launch time, smoothing is performed by assuming that the launch time is the first measurement time minus 25 s using (41). The corresponding RMSE, bias and STD of the LP estimate are shown in the last two columns of Table I. From Table I, it can be noticed that a small error in the launch time does not increase the position RMSE significantly. Even though the error in the launch time might affect the initial acceleration and jerk estimates, the launch time and the initial acceleration and jerk do not appear to be as vital as the launch position estimate.

6. CONCLUSION

In this paper, the launch point estimation of a ballistic target using the measurements from satellite-borne passive sensors during the boost phase of the target is considered. The target is assumed to have a two-stage boost phase with a free-flight phase between the two stages. A profile-free method with an adaptive model selection relying on the free-flight duration (assumed to be observed) is proposed for end-of-burnout and launch point estimation of ballistic targets. Measurements are assumed available only staring at a certain time after the launch. The launch point is estimated using smoothing followed by a least squares estimator. Prior information on the launch state such as zero initial velocity and zero (or known) altitude at launch are used to improve the estimate of the launch point.

From the simulation results as well as the PCRLB, it was observed that the launch point estimates were not improved by using measurements from the second stage of the boost phase. Hence, if the launch point estimate is the only item of interest, then there is no need for complicated filters like IMM to detect the maneuvers that occur after the time at which the accuracy of launch point estimate saturates. Also, the simulation results suggested that the exponentially autocorrelated acceleration model is not a good choice for launch point estimation and the Wiener process jerk model is the better.

APPENDIX. NOMENCLATURE

$E\{\cdot\}$	Expectation operator
F	State transition matrix
γ	Elevation
Q	Process noise covariance
h	Nonlinear measurement function
$\bar{H}$	Jacobian of nonlinear measurement function
$\bar{\bar{H}}$	Jacobian of stacked nonlinear measurement functions
J	Fisher information matrix
P	Covariance of the state estimate
R	Measurement error covariance
T	Sampling period
θ	Azimuth
$\mathbf{x}$	State vector
$\hat{\mathbf{x}}$	Estimate of state vector $\mathbf{x}$
$\mathbf{z}$	Measurement vector

REFERENCES

[1] Y. Bar-Shalom, P. K. Willett, and X. Tian
Tracking and Data Fusion.
Storrs, CT: YBS Publishing, 2011.

[2] Y. Bar-Shalom, X. Li, and T. Kirubarajan
Estimation with Applications to Tracking and Navigation.
New York: Wiley, 2001.

[3] A. Benavoij, L. Chisci, and A. Farina
Tracking of a ballistic missile with a-priori information.
IEEE Transactions on Aerospace and Electronic Systems, **43**, 3 (July 2007), 1000–1016.

[4] W. D. Blair, J. Lawton, and G. Martell
Private communication from NSWC Dahlgren Division, VA, 1995, 1997.

[5] N. J. Danis
Space-based tactical ballistic missile launch parameter estimation.
IEEE Transactions on Aerospace and Electronic Systems, **29**, 2 (Apr. 1993), 412–424.

[6] A. Farina, L. Timmoneri, and D. Vigilante
Classification and launch-impact point prediction of ballistic target via multiple model maximum likelihood estimator (MM-MLE).
In Proceedings of the IEEE Conference on Radar, Verona, NY, Apr. 2006.

[7] W. J. Farrell
Interacting multiple model filter for tactical ballistic missile tracking.
IEEE Transactions on Aerospace and Electronic Systems, **44**, 2 (Apr. 2008), 418–426.

[8] M. L. Hernandez, T. Kirubarajan, and Y. Bar-Shalom
Multisensor resource deployment using posterior Cramér-Rao bounds.
IEEE Transactions on Aerospace and Electronic Systems, **40**, 2 (Apr. 2004), 399–416.

[9] J. N. Holt and R. Fletcher
An algorithm for constrained nonlinear least squares.
Journal of the Institute of Mathematics and Its Applications, **23**, 4 (1979), 449–463.

[10] R. G. Hutchins and P. E. Pace
Studies in trajectory tracking and launch point determination for ballistic missile defense.
In Proceedings of SPIE Conference on Signal and Data Processing of Small Targets, 6236-0Y, Orlando, FL, Apr. 2006.

[11] X. R. Li and V. P. Jilkov
A survey of maneuvering target tracking—Part II: ballistic target models.
Proceedings of SPIE Conference on Signal and Data Processing of Small Targets, San Diego, CA, Aug. 2001.

[12] Y. Li, T. Kirubarajan, M. Yeddanapudi and Y. Bar-Shalom
Trajectory and launch point estimation for ballistic missiles based on boost-phase LOS measurements.
In Proceedings of the IEEE Aerospace Conference, Snowmass, CO, Mar. 1999, 425–442.

[13] L. N. Lillard, H. E. Evans, and J. J. Spaulding
Minimum variance missile launch and impact estimation by fusing observations from multiple sensors.
In Proceedings of the IEEE Aerospace Conference, 3, Aspen, CO, Feb. 1997, 309–320.

[14] V. P. S. Naidu, G. Girija, and J. R. Raol
Estimation of launch and impact points of a flight trajectory using U-D Kalman filter/smoother.
Defence Science Journal, **56**, 4 (Oct. 2006), 451–463.

[15] N. Nandakumaran, R. Tharmarasa, T. Lang, M. McDonald, and T. Kirubarajan
Interacting multiple model forward filtering and backward smoothing for maneuvering target tracking.
In Proceedings of SPIE Conference on Signal and Data Processing of Small Targets, 7445-03, San Diego, CA, Aug. 2009.

[16] E. Nelson, M. Pachter, and S. Musick
Projectile launch point estimation from radar measurements.
In Proceedings of the American Control Conference, 2, Portland, OR, June 2005, 1275–1282.

[17] R. W. Osborne, III and Y. Bar-Shalom
Statistical efficiency of composite position measurements from passive sensors.
In Proceedings of SPIE Conference on Signal Processing, Sensor Fusion and Target Recognition, 8050-07, Orlando, FL, Apr. 2011.

[18] P. W. Richards
Constrained Kalman filtering using pseudo-measurements.
In Proceedings of the IEE Colloquium on Algorithms for Target Tracking, London, UK, May 1995.

[19] M. Simandl, J. Kralovec, and P. Tichavsky
Filtering, predictive, and smoothing Cramer-Rao bounds for discrete-time nonlinear dynamic systems.
Automatica, **37** (2001), 1703–1716.

[20] H. Van Trees
Detection, Estimation and Modulation Theory, Vol. I.
New York: Wiley, 1968.

[21] J. R. Van Zandt
Boost phase tracking with an unscented filter.
In Proceedings of SPIE Conference on Signal and Data Processing of Small Targets, 4728, Orlando, FL, Apr. 2002, 263–274.

[22] P. Zarchan
Boost phase filtering options: is simpler better?
Submitted to *AIAA J-G&C*, 2010.

Ratnasingham Tharmarasa was born in Sri Lanka in 1975. He received the B.Sc.Eng. degree in electronic and telecommunication engineering from University of Moratuwa, Sri Lanka in 2001, and the M.A.Sc. and Ph.D. degrees in electrical engineering from McMaster University, Canada in 2003 and 2007, respectively.

From 2001 to 2002 he was an instructor in electronic and telecommunication engineering at the University of Moratuwa, Sri Lanka. During 2002–2007 he was a graduate student/research assistant in ECE department at the McMaster University, Canada. Currently he is working as a research associate in the Electrical and Computer Engineering Department at McMaster University, Canada. His research interests include target tracking, information fusion and sensor resource management.

Thiagalingam Kirubarajan (S'95—M'98—SM'03) was born in Sri Lanka in 1969. He received the B.A. and M.A. degrees in electrical and information engineering from Cambridge University, England, in 1991 and 1993, and the M.S. and Ph.D. degrees in electrical engineering from the University of Connecticut, Storrs, in 1995 and 1998, respectively.

Currently, he is a professor in the Electrical and Computer Engineering Department at McMaster University, Hamilton, Ontario. He is also serving as an Adjunct Assistant Professor and Associate Director of the Estimation and Signal Processing Research Laboratory at the University of Connecticut. His research interests are in estimation, target tracking, multisource information fusion, sensor resource management, signal detection and fault diagnosis. His research activities at McMaster University and at the University of Connecticut are supported by U.S. Missile Defense Agency, U.S. Office of Naval Research, NASA, Qualtech Systems, Inc., Raytheon Canada Ltd. and Defense Research Development Canada, Ottawa. In September 2001, Dr. Kirubarajan served in a DARPA expert panel on unattended surveillance, homeland defense and counterterrorism. He has also served as a consultant in these areas to a number of companies, including Motorola Corporation, Northrop-Grumman Corporation, Pacific-Sierra Research Corporation, Lockhead Martin Corporation, Qualtech Systems, Inc., Orincon Corporation and BAE systems. He has worked on the development of a number of engineering software programs, including BEARDAT for target localization from bearing and frequency measurements in clutter, FUSEDAT for fusion of multisensor data for tracking. He has also worked with Qualtech Systems, Inc., to develop an advanced fault diagnosis engine.

Dr. Kirubarajan has published about 100 articles in areas of his research interests, in addition to one book on estimation, tracking and navigation and two edited volumes. He is a recipient of Ontario Premier's Research Excellence Award (2002).

Nandakumaran Nadarajah (S'05—M'10) was born in Sri Lanka in 1976. He received the B.Sc.Eng. degree in electrical and electronic engineering from University of Peradeniya, Peradeniya, Sri Lanka, in 2001, and the M.A.Sc. and Ph.D. degrees in electrical engineering from McMaster University, Canada, in 2005 and 2009, respectively.

From 2002 to 2003 he was an assistant lecturer in Electrical and Electronic Engineering at the University of Peradeniya. From 2003 to 2009 he was a graduate student/research assistant in Electrical and Computer Engineering Department at McMaster University, Canada. Currently, he is working as a postdoctoral research fellow at Curtin University, Perth, Australia. His research interests are in signal processing, target tracking, data fusion, GNSS navigation and attitude determination.

Yaakov Bar-Shalom (S'63—M'66—SM'80—F'84) was born on May 11, 1941. He received the B.S. and M.S. degrees from the Technion, Israel Institute of Technology, in 1963 and 1967 and the Ph.D. degree from Princeton University, Princeton, NJ, in 1970, all in electrical engineering.

From 1970 to 1976 he was with Systems Control, Inc., Palo Alto, CA. Currently he is Board of Trustees Distinguished Professor in the Department of Electrical and Computer Engineering and Marianne E. Klewin Professor in Engineering. He is also director of the ESP Lab (Estimation and Signal Processing) at the University of Connecticut. His research interests are in estimation theory and stochastic adaptive control and he has published over 360 papers and book chapters in these areas. In view of the causality principle between the given name of a person (in this case, "(he) will track," in the modern version of the original language of the Bible) and the profession of this person, his interests have focused on tracking.

He coauthored the monograph *Tracking and Data Association* (Academic Press, 1988), the graduate text *Estimation with Applications to Tracking and Navigation* (Wiley, 2001), the text *Multitarget-Multisensor Tracking: Principles and Techniques* (YBS Publishing, 1995), and edited the books *Multitarget-Multisensor Tracking: Applications and Advances* (Artech House, Vol. I 1990; Vol. II 1992, Vol. III 2000). He has been elected Fellow of IEEE for "contributions to the theory of stochastic systems and of multitarget tracking." He has been consulting to numerous companies, and originated the series of Multitarget Tracking and Multisensor Data Fusion short courses offered at Government Laboratories, private companies, and overseas.

During 1976 and 1977 he served as associate editor of the *IEEE Transactions on Automatic Control* and from 1978 to 1981 as associate editor of *Automatica*. He was program chairman of the 1982 American Control Conference, general chairman of the 1985 ACC, and cochairman of the 1989 IEEE International Conference on Control and Applications. During 1983–1987 he served as chairman of the Conference Activities Board of the IEEE Control Systems Society and during 1987–1989 was a member of the Board of Governors of the IEEE CSS. Currently he is a member of the Board of Directors of the International Society of Information Fusion and served as its Y2K and Y2K2 President. In 1987 he received the IEEE CSS distinguished Member Award. Since 1995 he is a distinguished lecturer of the IEEE AESS. He is corecipient of the M. Barry Carlton Awards for the best paper in the *IEEE Transactions on Aerospace and Electronic Systems* in 1995 and 2000, and received the 1998 University of Connecticut AAUP Excellence Award for Research, the 2002 J. Mignona Data Fusion Award from the DoD JDL Data Fusion Group, and the 2008 IEEE D. J. Picard Medal for Radar Technologies and Applications.

Thayananthan Thayaparan earned a B.Sc. (Hons.) in physics at the University of Jaffna, Srilanka in 1987, an M.Sc. in physics at the University of Oslo, Norway in 1991, and a Ph.D. in atmospheric physics at the University of Western Ontario, Canada in 1996.

From 1996 to 1997, he was employed as a postdoctoral fellow at the University of Western Ontario. In 1997, he joined the Defence Research and Development Canada–Ottawa, Department of National Defence, Canada, as a defence scientist. His research interests include advanced radar signal and image processing methodologies and techniques against SAR/ISAR and HFSWR problems such as detection, classification, recognition, and identification. His current research includes computational synthetic aperture radar imaging algorithms, time-frequency analysis for radar detection, imaging and signal analysis, radar micro-Doppler analysis, and concealed weapon detection using radars.

Dr. Thayaparan is currently serving in the Editorial Board of IET Signal Processing. He has authored or coauthored over 170 publications in journals, proceedings, and internal distribution reports. He is a fellow of the IET (previously IEE). He has been appointed as an adjunct professor at McMaster University.